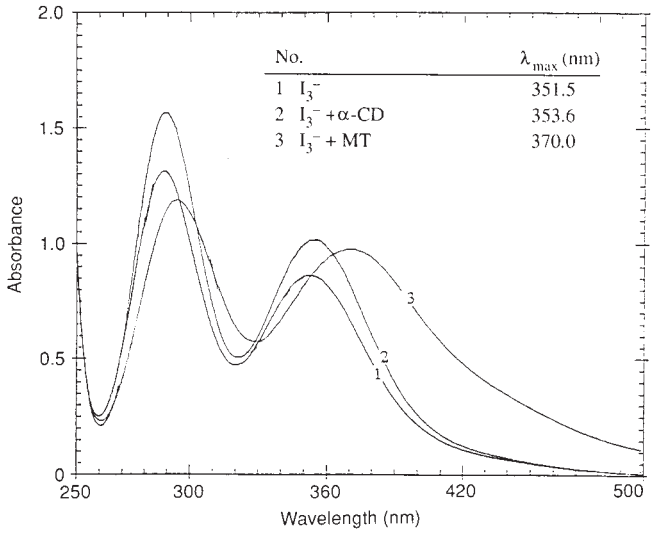

FIG. 5 The absorption spectra of KI-I_2 solutions in the absence (1) and presence (2) of α-CD (0.4 g l^{-1}) and presence (3) of molecular tube (MT) (0.4 g l^{-1}). $[I_3^-] = 2.0 \times 10^{-4}$ M. Cell length is 1 cm.

is less than 20,000. This value is consistent with the fact that the molecular mass of the molecular tube, prepared from PEG of molecular mass 1,450, is ~17,000. Therefore, intrachain crosslinking took place predominantly. The yield of the final product is 92%. Its elemental analysis gave the following results: found (calculated with three crosslinking bridges between CDs for $C_{45}H_{72}O_{33}(H_2O)_2$): C, 45.88 (45.92); H, 6.67 (6.51).

The product was soluble in water, dimethylformamide (DMF), and dimethylsulphoxide (DMSO), although polyrotaxanes are insoluble in water and DMF, and soluble in DMSO. The product was characterized by ^{1}H NMR, ^{13}C NMR, infrared and ultraviolet spectroscopy, and gel permeation chromatography. Figure 4 shows the ^{1}H NMR spectra of the molecular tube in D_2O and in DMSO-d_6. The ^{1}H NMR and ^{13}C NMR spectra show that CD, the bridge, and the H_1 proton with the bridge can be observed. All the peaks of the ^{1}H NMR spectrum are broadened, indicating the product is polymeric.

When the solution of the molecular tube was added to a pale yellow solution of potassium iodide containing free iodine (KI-I_2), a deep red colour was instantaneously produced, although the addition of an α-CD solution to KI-I_2 solution caused no colour change. Figure 5 shows the absorption spectra of KI-I_2 solution in the presence and absence of α-CD and molecular tube. On addition of α-CD, the position of the absorption maximum changed little, with some increase in intensity. On addition of the molecular tube solution, the absorption maximum shifted to longer wavelength and a large tailing over 500 nm was observed. On addition of randomly crosslinked α-CD with epichlorohydrin, no visible changes took place. These results indicate that I_3^- ions are arranged linearly in the tube. The shift is not so large compared with that observed with amylose and KI-I_2 solution, but is similar to that observed with amylopectin. The change in the spectrum was found to be a maximum at a ratio of CD unit to I_3^- molecule of 1 : 1. These findings indicate that such template synthesis provides an approach to the construction of new nanostructures. □

Received 26 April; accepted 18 June 1993.

1. Whitesides, G. M., Mathias, J. P. & Seto, C. T. *Science* **254,** 1312–1319 (1991).
2. Iijima, S. *Nature* **354,** 56–58 (1991).
3. Ajayan, P. M. & Iijima, S. *Nature* **361,** 333–334 (1993).
4. Bender, M. L. & Komiyama, M. *Cyclodextrin Chemistry* (Springer, Berlin, 1978).
5. Pregel, M. J., Jullen, L. & Lehn, J.-M. *Angew. Chem. int. Edn. engl.* **31,** 1637–1640 (1992).
6. Harada, A., Li, J. & Kamachi, M. *Nature* **356,** 325–327 (1992).
7. Wenz, G. & Keller, B. *Angew. Chem. int. Edn. engl.* **31,** 197–198 (1992).
8. Gibson, H. W. & Marand, H. *Adv. Mat.* **5,** 11–21 (1993).

Annual growth banding in a cave stalagmite

Andy Baker*†, Peter L. Smart*, R. Lawrence Edwards† & David A. Richards*†

* Department of Geography, University of Bristol, Bristol BS8 1SS, UK
† Minnesota Isotope Laboratory, Department of Geology and Geophysics, University of Minnesota, Minneapolis, Minnesota 55455, USA

THE presence of microscopic luminescence banding in cave calcite deposits (speleothems) has recently been reported[1–3]. The luminescence seems to be caused by excitation of humic and fulvic acids derived from the overlying soil and subsequently incorporated into the calcite[3,4]. We have tested whether such luminescence corresponds to annual growth layers, using high-precision thermal-ionization mass-spectrometric ^{238}U–^{234}U–^{230}Th ages from banded sections of a Holocene stalagmite. We report here that the timespans yielded by counting bands, on the assumption that they are annual, agree within error limits with those obtained by our uranium–thorium dating. This demonstration that the banding is annual should make banded speleothems valuable resources for providing high-resolution records of past climate (in which precipitation can be estimated from growth rates[5,6] and temperatures from stable-isotope measurements[7]) and solar–terrestrial correlations (as the luminescence intensity can be related to the solar sunspot cycle[1–3]).

Forty-three speleothem samples were collected from karst areas in the United Kingdom. After cutting along the axis of growth, 2-mm-thick polished sections were prepared. These were observed under a standard Zeiss microscope fitted with an IV Fl epi-fluorescence condenser containing a 50 W super-pressure mercury lamp. A 320–420 nm excitation filter was used to transmit the portion of ultraviolet light known to generate a strong luminescence from organic matter (around 350–380 nm; ref. 4), and the luminescence itself viewed using a 420-nm barrier filter, which prevented transmission of the excitation waveband. A magnification of between ×64 and 100 was used to observe luminescence, which was recorded using long-exposure photography on high-contrast Kodalith Ortho 6556 (type 3) film. This was then scanned to give a digitized image. A 5 pixel (125 μm) smoothing filter was then applied to remove noise, permit clear separation of consecutive bands, and allow measurement of peak to peak bandwidth. Assuming that the distance between successive peaks represents the annual growth of the sample, the average axial growth rate can then be determined.

Banding occurred only in a few samples (5 out of 43 examined). This may be due to the use of a mercury lamp source, which has a low-energy broad spectrum output, and may not be powerful enough to excite weak luminescence banding. Although Shopov *et al.* used an ultraviolet laser source, they also noted that annual banding was apparently absent in some samples[2]. The limited preservation of annual banding may be related to strict requirements on the type of percolation flow feeding the speleothem; soil water and unsaturated zone storage need to be adequate to maintain flow during the summer, while residence times overall remain sufficiently short that summer and winter waters are not completely mixed. Crystal structure and orientation also appear to be important factors in signal preservation, but further investigation is needed. Finally, it would also be useful to compare the luminescence record with that of visible banding, which has occasionally also been reported in speleothem[8,9].

TABLE 1 Uranium/thorium isotopic data and mass-spectrometric ages for SU-80-11

Sample name*	Distance down axis*	^{238}U concentration ng g^{-1}	$^{234}U/^{238}U$ $\times10^{6}$	$^{230}Th/^{232}Th$ $\times10^{-6}$	$\delta^{234}U(0)$†‡ ‰	$\delta^{234}U(T)$†‡ ‰	$[^{230}Th/^{238}U]_{act}$§‖	Age ‡ years BP	Corrected age¶ years BP
SU-80-11A	2 mm	247.61±0.75	64.64±0.36	26.3±0.9	181.2±6.6	185.7±6.8	0.0878±0.0029	8,340±290	6,970±750
SU-80-11B	28 mm	254.76±0.75	64.38±0.43	110.1±3.0	176.5±7.8	179.0±7.9	0.0506±0.0014	4,730±130	4,540±160
SU-80-11C	64 mm	237.11±0.48	66.84±0.27	148.7±4.5	221.4±4.9	223.6±5.0	0.0378±0.0011	3,370±100	3,270±110
SU-80-11D(1)	80 mm	329.49±0.30	65.97±0.12	149.9±2.3	205.6±2.1	207.4±2.2	0.0339±0.0005	3,103±43	3,014±62
SU-80-11D(2)		329.56±0.24	65.90±0.11	147.0±6.5	204.4±2.1	206.2±2.1	0.0333±0.0014	3,051±131	2,962±138
SU-80-11E	96 mm	302.95±1.11	67.31±0.31	1622±95	230.1±5.6	231.9±5.7	0.0304±0.0008	2,680±70	2,670±70

* Sample location and distances shown in Fig. 1; SU-80-11D(1) and SU-80-11D(2) are replicate analyses of different aliquots of the solution derived from sample SU-80-11D.

† $\delta^{234}U=([(^{234}U/^{238}U)/(^{234}U/^{238}U)eq]-1)\times10^{3}$, where $(^{234}U/^{238}U)eq$ is the atomic ratio at secular equilibrium and is equal to 5.472×10^{-5}. $\delta^{234}U(0)$ is the measured value. $\delta^{234}U(T)$ is the initial value and is equal to $\delta^{234}U(0)e^{\lambda_{234}T}$.

‡ Values for decay constants are $\lambda_{238}=1.551\times10^{-10}\ yr^{-1}$ (ref 15), $\lambda_{234}=2.835\times10^{-6}\ yr^{-1}$ (refs 16, 17), and $\lambda_{230}=9.195\times10^{-6}\ yr^{-1}$ (ref 18).

§ Calculated from the atomic $^{230}Th/^{238}U$ ratio by multiplying by $\lambda_{230}/\lambda_{238}$.

‖ Ages are calculated using $[^{230}Th^{238}U]act-1=e^{-\lambda_{230}T}+(\delta^{234}U(0)/1000)(\lambda_{230}/\lambda_{230}-\lambda_{234})(1-e^{-(\lambda_{230}-\lambda_{234})T})$ where T is the age in years.

¶ Corrected ages assume an initial $^{230}Th/^{232}Th$ atomic ratio of $4.4\pm2.2\times10^{-6}$ (method 1, equation 8 from ref. 19). This is the value for a material at secular equilibrium, with a crustal $^{232}Th/^{238}U$ value of 3.8. The error is arbitrarily assumed to be 50%. The error in the corrected age for SU-80-11A is large because of detrital contamination and the uncertainty in the initial $^{230}Th/^{232}Th$ ratio used in correcting for this contamination.

The Holocene stalagmite SU-80-11, collected from Uamh an Tartair Cave, Sutherland (NW Scotland), was found to contain dense luminescence banding at irregular intervals along its length, an example of which is shown in Fig. 1. This banding was not continuously preserved down the section, with the longest unbroken record covering 36 years. Figure 2 presents the complete record of bandwidths obtainable along the growth axis in the form of the mean and standard deviation of sets of five consecutive bands. Along the two portions of the sample for which luminescent bands were visible (1 and 2 on Fig. 2), the growth rates are 0.0549 ± 0.0027 mm yr^{-1} and 0.0565 ± 0.0029 mm yr^{-1} (2 s.e.m.; number of bands, $n=242$ and 66, respectively). The mean growth rates do not vary significantly for the two intervals, whereas inter-annular variability is of a magnitude comparable to that of present annual precipitation variations (work in progress).

The development of high-precision thermal-ionization mass-spectrometric ^{238}U–^{234}U–^{230}Th (TIMS ^{230}Th) dating[10–12] and its application to speleothems[13] provides a precise means of testing the growth rate of the intervals with luminescence banding. Using a diamond wire saw, five sub-samples (A–E) of less than 2 g weight were cut from SU-80-11 for TIMS ^{230}Th dating (Fig. 1). Analytical methods are described in refs 10–12, but modified for use on a Finnigan-MAT 262-RPQ mass spectrometer, which is optimized for measuring small ion beams. Ion counting techniques with low dark noise combined with high-abundance sensitivity allowed SU-80-11 to be dated despite low levels of ^{230}Th (380 to 960 million atoms per g of speleothem) and relatively low $^{230}Th/^{232}Th$ (26.3 to $1{,}622\times10^{-6}$). ^{230}Th ion currents, measured on the multiplier before the (unused) quadrupole second stage, ranged from 10 to 20 c.p.s.; 3,000 to 9,000 ^{230}Th ions were counted in each mass spectrometer run. Within-run statistics were comparable to counting statistics. The TIMS ^{230}Th ages obtained are listed in Table 1. Replicate analyses agree within error indicating that the analyses are reproducible. The ages are also consistent with their stratigraphic positions within the speleothem.

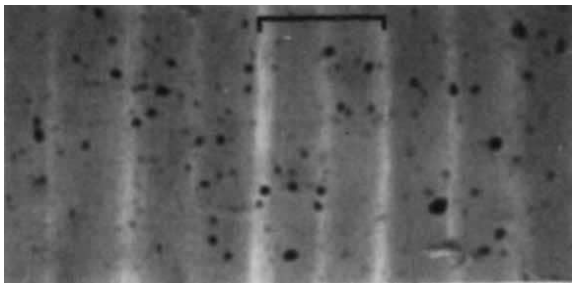

FIG. 1 Photomicrograph of luminescent banding 85 mm from base of sample (approximate age, 2,950±150 years). Nine consecutive bands are visible under microscope magnification of ×100. Black spots are dust particles entrapped within the UV apparatus, and are not a feature of the speleothem. Scale bar, 0.1 mm.

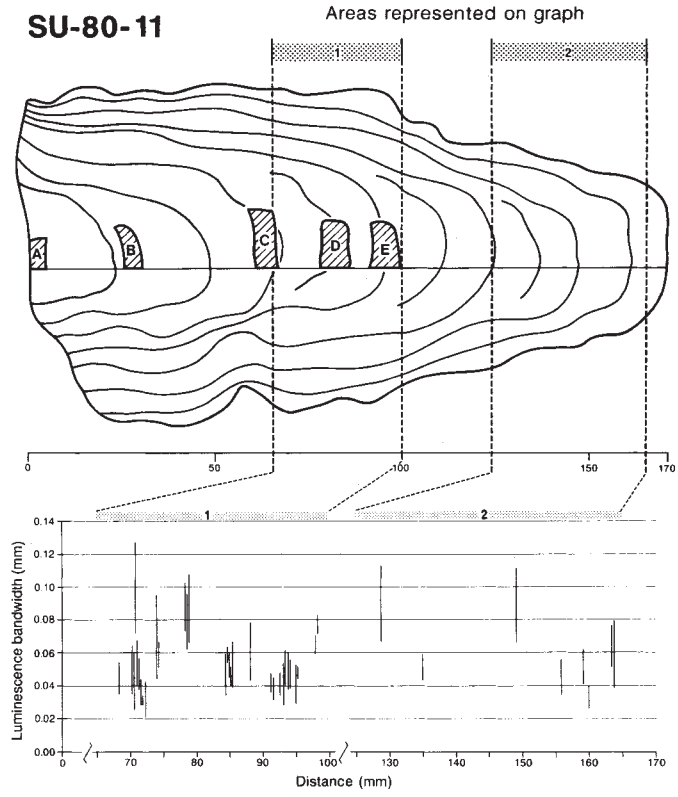

FIG. 2 SU-80-11, showing position of samples for TIMS ^{230}Th dating and luminescence bandwidth record. Bandwidth equals growth rate (mm yr^{-1}) if banding is annual. Because of the large number of bands observed, data is only presented where five consecutive luminescence bands occur; the length of each bar representing $\pm1\sigma$ of the population of the five-band set, and the centre the arithmetic mean.

The sample grew during a period when climatic conditions changed relatively little in the UK (the late climatic optimum)[14]. Deposition appears to be continuous in SU-80-11 with no growth hiatuses visible, thus absolute growth rates can be calculated between sub-samples. There is a general increase in growth

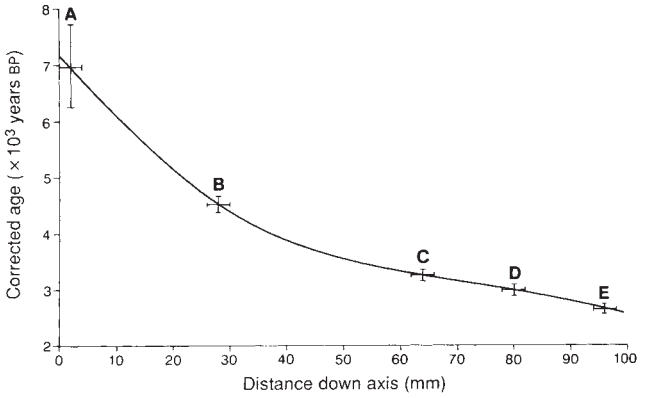

FIG. 3 Graph of TIMS ^{230}Th ages against distance up the growth axis of SU-80-11. The gradient of the curve is equivalent to the growth rate, and shows a slow decrease in growth rate with time.

rate over time, but between samples C and E (interval 1), growth rate is constant (Fig. 3). These samples span a 32-mm section of the stalagmite for which the luminescence record also allows determination of a growth rate (assuming annual banding) of 0.0549 ± 0.0027 mm yr^{-1} (2 s.e.m.; $n = 242$). This gives an age difference between sub-samples C and E of 586 ± 28 years, which compares with a difference of 600 ± 130 years derived from the TIMS ^{230}Th ages (Table 1 and Fig. 3). The difference between these is well within the 2σ analytical uncertainty associated with the two estimates, and it can be concluded that the luminescence banding is indeed annual in nature.

Luminescence banding in speleothems, here demonstrated for the first time by TIMS ^{230}Th dating to be annual, can be used to provide an annual signal for high-resolution palaeoclimatic studies. First, as suggested by previous workers[1–3], annual variations of intensity of the luminescence may provide information on changes in solar output. They demonstrated that one flowstone sample showed peaks in luminescence intensity with a periodicity of 0.95, 8.6, 10.4 and 13.3 bandwidths. These were thought to be caused by variations in plant productivity associated with both the annual temperature cycle (0.95 bandwidth) and the 11-year sun-spot cycle (8.6, 10.4 and 13.3 bandwidths). Second, the distance between bands can be used to provide measures of growth rate variation. As shown by this sample, significant variations in growth rate occur, and may be influenced by both temperature and precipitation, as theoretically modelled by Dreybrodt[5,6]. The potential of this palaeoclimate signal is currently under assessment, and may provide a unique proxy record of palaeoprecipitation. Furthermore, the banding itself can be used as a high resolution chronostratigraphic tie between TIMS ^{230}Th ages, and other high-resolution records obtainable from speleothems (trace elements, oxygen and carbon isotopes)[7]. □

Received 25 September 1992; accepted 17 June 1993.

1. Shopov, Y., Dermendjiev, V. & Buyukliev, G. *Proc. Int. Cong. Speleol. Hung.* **10,** 95–97 (1989).
2. Shopov, Y., Dermendjiev, V. & Buyukliev, G. *Proc. Int. Conf. Envir. Changes Karst Areas, Padova, Italy,* 17–22 (1991).
3. Shopov, Y. & Dermendjiev, V. *C. r. Acad. Bulg. Sci.* **43,** 9–12 (1990).
4. White, W. B. & Brennan, E. S. *Proc. Int. Cong. Speleol.* **10,** 212–214 (1989).
5. Buhmann, D. & Dreybrodt, W. *Chem. Geol.* **48,** 189–211 (1985).
6. Dreybrodt, W. *Processes in Karst Systems* (Springer, Berlin, 1988).
7. Schwarcz, H. P. in *Handbook of Environmental Isotope Geochemistry* Vol. 2 (eds Fritz, P. & Fontes, J. C.) 271–303 (Elsevier, Amsterdam, 1986).
8. Broecker, W. S., Olson, E. A. & Orr, P. C. *Nature* **185,** 93–94 (1960).
9. Orr, P. C. *Santa Barbara Museum of Natural History, Anthropology Department, Bulletin No. 1.* 19pp (Santa Barbara Museum of Natural History, California, 1952).
10. Chen, J. H., Edwards, R. L. & Wasserburg, G. J. *Earth planet. Sci. Lett.* **80,** 241–251 (1986).
11. Edwards, R. L., Chen, J. H. & Wasserburg, G. J. *Earth planet. Sci. Lett.* **81,** 175–192 (1987).
12. Edwards, R. L., Chen, J. H., Ku, T.-L. & Wasserburg, G. J. *Science* **236,** 1547–1553 (1987).
13. Li, W.-X. *et al. Nature* **339,** 534–536 (1989).
14. Simmons, I. G., Dimbleby, G. W. & Grigson, C. in *The Environment in British Prehistory* (eds Simmons, I. G. & Tooley, M. J.) 82–124 (Duckworth, London, 1981).
15. Jaffey, A. H., Flynn, K. F., Glendenin, L. W., Bently, W. C. & Essling, A. M. *Phys. Rev.* C**4,** 1889–1906 (1971).
16. de Bievre, P. *et al.* in *Proc. Int. Conf. Nuclear Data Measurement and Applications* (ed. Hurrell, M. L.) 221–225 (Institute of Civil Engineers, London, 1971).
17. Lounsbury, M. & Durham, R. W. in *Proc. Int. Conf. Nuclear Data Measurement and Applications* (ed. Hurrell, M. L.) 215–219 (Institute of Civil Engineers, London, 1971).
18. Meadows, J. W., Armani, J., Callis, E. L. & Essling, A. M. *Phys. Rev.* C**2,** 750–754 (1980).
19. Schwarcz, H. P. *Archaeometry* **22,** 3–24 (1980).

ACKNOWLEDGEMENTS. We thank Y. Shopov and D. C. Ford at McMaster University for stimulating initial enthusiasm in luminescence banding, M. Cheshire (UV apparatus, Bristol), T. Philpott (photography), S. Godden (diagrams), W. Beck (mass-spectrometry) and C. Kidd (digitising). A.B. was funded by a NERC studentship. The TIMS work was funded by US National Science Foundation grants (to the University of Minnesota), the McKnight foundation and the University of Minnesota.

Blueschist metamorphism in an active subduction zone

Hirokazu Maekawa*, Masaya Shozui*†, Teruaki Ishii‡ Patricia Fryer§ & Julian A. Pearce‖

* Department of Earth and Planetary Sciences, Faculty of Science, Kobe University, Nada, Kobe 657, Japan
‡ Ocean Research Institute, University of Tokyo, Nakano, Tokyo 164, Japan
§ Department of Geology and Geophysics, University of Hawaii at Manoa, 2525 Correa Rd, Honolulu, Hawaii 96822, USA
‖ Department of Geological Sciences, University of Durham, Durham DH1 3LE, UK

THE high-pressure, low-temperature metamorphic rocks known as blueschists have long been considered to form in subduction zones, where the descent of a relatively cold slab leads to the occurrence of unusually low temperatures at mantle pressures. Until now, however, the link between blueschist-facies rocks and subduction zones has been indirect, relying on a spatial association of blueschists with old subduction complexes, and estimates of the geothermal gradients likely to exist in subduction zones. Here we strengthen this link, by reporting the discovery of blueschist-facies minerals (lawsonite, aragonite, sodic pyroxene and blue amphibole) in clasts from a serpentinite seamount in the forearc of the active Mariana subduction zone. The metamorphic conditions estimated from the mineral compositions are 150–250 °C and 5–6 kbar (16–20 km depth). The rocks must have been entrained in rising serpentine mud diapirs, and extruded from mud volcanoes onto the sea floor. Further study of these rocks may provide new insight into the tectonics of trench-forearc systems, and in particular, the processes by which blueschist-facies clasts come to be associated with forearc sediments in ancient subduction complexes.

During Ocean Drilling Program Leg 125, scientists drilled two serpentinite seamounts in the Mariana and Izu-Bonin forearcs[1]. They recovered abundant serpentinized peridotites and minor amounts of low-grade metamorphosed mafic rocks from both seamounts. The mineral assemblages and chemistries show that a bimodal pressure assemblage is represented within these low-grade metamorphic rocks: one at low, and one at high pressure[2]. The high-pressure assemblage, containing blueschist-facies minerals, was present only in one hole at ODP Site 778 in the Mariana forearc.

Hole 778A was drilled to a depth of 107.6 metres below the sea floor (m.b.s.f.) on the southern flank of Conical Seamount. This seamount is located in the Mariana forearc, ~80 km west of the trench axis (Fig. 1). The drill core contained ~60 metamorphosed mafic rocks as subrounded pebble-size clasts in a serpentine matrix. These protoliths were mainly aphyric to fine-grained basalt and amphibolite, althouth later-stage cataclastic deformation and chloritization usually obliterate the primary textures and obscure their origin.

Nine specimens of different lithologies from Hole 778A were

† Present address: Institute of Advanced Business Systems, Hitachi Ltd, 890 Kashimada, Saiwai, Kawasaki 211, Japan.